Electronic structure, Mechanical and Thermodynamic properties of CoYSb (Y= Cr, Mo, W) half-Heusler compounds as potential spintronic materials

O. T. Uto
Federal University of Agriculture
J. O. Akinlami
Federal University of Agriculture
S. Kenmoe (stephane.kenmoe@uni-due.de)
University of Duisburg-Essen
G. A. Adebayo
Federal University of Agriculture

Research Article

Keywords: nearly half-metal, Spin-polarization, Poisson's ratio, thermodynamic properties, Electronic band Structure

Posted Date: November 30th, 2021

DOI: https://doi.org/10.21203/rs.3.rs-1033376/v2

Electronic structure, Mechanical and Thermodynamic properties of CoYSb (Y= Cr, Mo, W) half-Heusler compounds as potential spintronic materials

O. T. Uto[a,1], P. O. Adebambo[a,1], J. O. Akinlami[a], S. Kenmoe[b,1] and G. A. Adebayo[a,1]

[a] *Department of Physics, Federal University of Agriculture, P.M.B. 2240, Abeokuta, Nigeria*

[b] *Department of Theoretical Chemistry, University of Duisburg-Essen, Universitätsstr. 2, D-45141 Essen, Germany*

Abstract

We used Density Functional Theory (DFT) calculations to investigate the structural, electronic, magnetic, mechanical and thermodynamic properties of CoYSb (Y = Cr, Mo and W) compounds. These are XYZ type half-Heusler alloys, which also exist in the face centred cubic MgAgAs-type structure and conform to $F\bar{4}3m$ space group. We computed these properties in three different atomic arrangements known as Type-I, Type-II and Type-III phases. In all these phases, the alloys were found to be in the ferromagnetic state. Furthermore, the calculated electronic band structure and the total electronic density of states indicated a metallic behaviour in CoWSb, nearly half-metallic in CoMoSb and half-metallic in CoCrSb, with a minority-spin band gap of 0.81 eV. Furthermore, the calculated mechanical properties predicted an anisotropic behaviour of these alloys in their stable phase. Finally, due to its high Debye temperature value, CoCrSb shows stronger covalent bonding than CoMoSb and CoWSb, respectively.

Keywords: nearly half-metal, Spin-polarization, Poisson's ratio, thermodynamic properties, Electronic band Structure

[1]authors to whom correspondence can also be sent: uto@physics.unaab.edu.ng, stephane.kenmoe@uni-due.de and adebayo@physics.unaab.edu.ng

1. Introduction

Ternary half-Heusler (HH) compounds involving Co-atom have recently attracted attention due to their high curie temperature and structural similarity with binary semiconductors with zinc-blende (ZB) structure that makes them potential candidates in optoelectronic and spintronic applications such as quantum sensors, resistors and computers devices[1]-[4], topological insulators [5]-[6], and thermoelectric devices [7], [14]. The wide range of usage of HH in applications is due to its excellent electrical, mechanical and electronic properties as well as thermal stability.

The crystal structure, $C1_b$, of any HH alloy is similar to the structure, $L2_1$, of a full-Heusler alloy (X_2YZ) but missing one X atom. The absence of inversion symmetry due to an empty X site and the low coordination number of the d-band metals in the HH alloys are believed to be essential for these materials novel electronic and magnetic properties. Some research groups have reported three possible distinct atomic arrangements, called Type-I, Type-II, and Type-III phases, due to this missing X atom in the HH alloy [1], [8]-[18].

Using Density Functional Theory, some Co-based HH compounds have been predicted to be semiconductor, metallic and half-metallic depending on the valence electron count (VEC) of the alloys[7], [23]-[18]. Nanda and Dasgupta [13] reported CoMoSb to be metallic from the series of HH compounds XMZ (X=Fe, Co, Ni: M=Ti, V, Nb, Zr, Cr, Mo, Mn and Z=Sb, Sn) they investigated. Zhong-Yu *et al.* [16] studied the structural and electronic properties of CoCrZ (Z= Sb and Te) using the full-potential linearized augmented plane wave(FP-LAPW) method. They showed that CoCrSb is half-metallic and has a spin-minority gap.

In this paper, we have investigated the structural,electronic, magnetic, mechanical and thermodynamics properties of a series of half-Heusler compounds, CoYSb (Y=Cr, Mo, W). We identify the most stable phases and investigate the impact of the lattice parameter on the magnetic properties for each stable phase of HH CoYSb (Y=Cr, Mo, W). To shed some light on the metallic behaviour, electronic transport, mechanical stability and strength of chemical bonding between their atoms, we have computed and analyzed the electronic spin bands and spin density of states (DOS), the response to shear deformation and unidirectional compression and the Debye temperature

2. computational details

Our calculations were performed using the Quantum Espresso *Ab-Initio* simulation package [24]-[26]. The generalized gradient approximation (GGA) within the Perdew-Burke-Ernzerhof (PBE) formulation [27] was used to treat elevctronic exchange and correlation effects. The plane wave energy cutoff was set to 680 eV and a k-point mesh of the Monkhorst-Pack type[30] and with $14 \times 14 \times 14$ grid was used to sample the irreducible Brillioun zone. For electronic properties calculations (band structure and DOS), a denser mesh grid $20 \times 20 \times 20$ was used. The Plane-waves pseudopotential (PWPP) basis functions set consists of the $3d^7\ 4s^2$, $3d^5\ 4s^1$, $4d^5\ 5s^1$, $5d^7\ 6s^2$ and $5s^2\ 5p^3$ for Co, Cr, Mo, W and Sb, respectively. The Thermo_pw code [28], [29] was used to calculate the mechanical and thermodynamic properties.

3. Results

3.1. Structural Properties

We started by calculating the equilibrium lattice constant of the HH compound CoYSb (Cr, Mo, W) considering the three possible site arrangement of X and Y atoms shown in fig 1.

[a] [b] [c]

Figure 1: The optimized crystal structure of CoYSb (Y=Cr, Mo and W) for (a) Type-I (b) Type-II and (c) Type-III. In Table 1, the Wyckoff [19] positions of atoms and vacancies are given. The alloys have been studied in Type-I, Type-II and Type-III phases which conform to $F\bar{4}3m$ space group.

Fig. 2 shows the energy–volume curves of the considered systems plotted by fitting to Murnaghan equation of states [20]. From there, the equilibrium lattice constant (a_o), bulk modulus (B), the minimum energy (E_{min})and pressure derivative (B') were derived and are reported in Table 2. The minimum energies obtained from the fitted energy–volume curves of CoYSb (Y = Cr, Mo, W) alloys show that the Type-I phase is the most stable structural phase

Table 1: The Wyckoff positions of the three atoms, X, Y, and Z: 4a = (0, 0, 0) a, 4b = (0.5, 0.5, 0.5) a and 4c = (0.25, 0.25, 0.25) a, with the 4d site vacant

Structural phase	**X**	**Y**	**Z**
Type I	4c	4b	4a
Type II	4b	4a	4c
Type III	4a	4c	4b

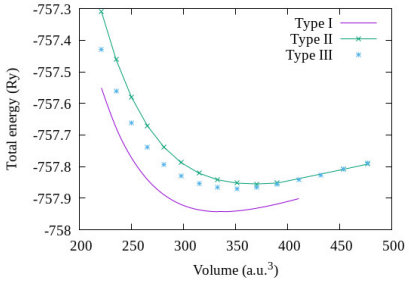

[a]

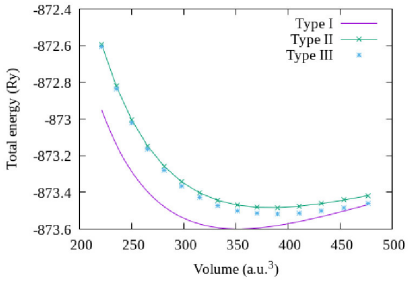

[b]

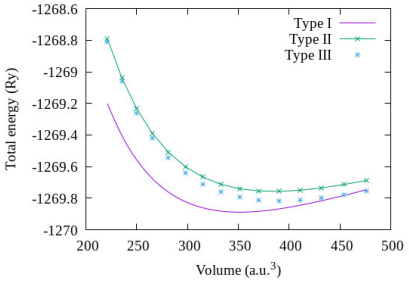

[c]

Figure 2: Calculated total energy as a function of volume in ferromagnetic state for the three possible structural phases (a) CoCrSb (b) CoMoSb and (c) CoWSb respectively.

(Fig.1 and Table 2). Also, the lattice constants are smaller in this phase and bulk moduli more significant than in other structural phases. However, large pressure derivatives of bulk moduli are observed in all structural phases, which indicates that these alloys display strong sensitivity against pressure change. Henceforth, all other results were obtained based on the stable state Type-I CoYSb phase apart from the magnetic properties.

Table 2: The optimized lattice constants, a_o (Å), equilibrium energies, E_{min} (Ry), bulk modulus, B (GPa) and pressure derivative for the bulk modulus, B' for CoYSb (Y= Cr, Mo, W) for the three possible structural phases.

Alloys	**Calculations**	**Structural phase**	a_o **(Å)**	**B (GPa)**	**B'**	E_{min} **(Ry)**
CoCrSb	This work	Type I	5.848	121.4	4.66	-757.944
	other calculations		5.79[a]			
			5.820[b]	135.4[b]		
			5.800[c]			
		Type II	6.031	97.6	4.33	-757.856
		Type III	5.935	98.6	4.71	-757.869
			5.935[d]			
CoMoSb		Type I	5.937	152.2	4.62	-873.598
	other calculations		5.935[d]			
		Type II	6.134	124.1	4.13	-873.484
		Type III	6.140	131.6	3.94	-873.520
CoWSb		Type I	5.939	164.9	4.32	-1269.888
		Type II	6.133	138.7	4.01	-1269.758
		Type III	6.145	148.2	3.81	-1269.819

a Ref.[14]
b Ref.[15]
c Ref.[16]
d Ref.[13]

3.2. Magnetic Properties

The calculated total and partial magnetic moments for all phases are listed in Table 3. It is seen that for CoCrSb, irrespective of the structural phase, the major contribution to the total magnetic moment comes from the Y (Cr) atom. Whereas, for the other two materials, i.e. CoYSb (Y = Mo and W), it is only in the Type-I phase that the major contributors to

the magnetic moment come from the Y atom. As shown in Table 3, their primary contributions come from Co-atom for the structural phases Type-II and Type-III phases. This discrepancy is attributed to the higher lattice parameters as well as unstable phases in the atomic positions for Type-II and Type-III used in the calculations. However, irrespective of the structural phase, the total magnetic moments for CoYSb (Y = Cr, Mo and W) are greater than 1, which indicates that these materials have ferromagnetic properties.

Many half-Heusler alloys follow the Slater-Pauling (SP) rule M_t=Z_t –18 [31], [32] where Z_t is the total number of valence electrons and 18 means that there are 9 electrons occupied spin-down states per unit cell. CoMoSb and CoWSb, just like CoCrSb alloy, have 20 valence electrons, indicating that the total magnetic moment M_t should be 2 μ_B. For our calculated values, this is in accord only with Type-I alloys. Although, the magnetic moment increase by 0.1 μ_B and 0.49 μ_B for CoCrSb and CoWSb respectively. Whereas it is reduced by 0.21 μ_B for CoMoSb alloy. This slight discrepancy is attributed to the position at the Fermi level. For CoCrSb and CoWSb, the pseudogap is slightly below the Fermi level, while for CoMoSb, the pseudogap is slightly higher than the Fermi level. These results are compared with the work of Galanakis and Dederichs [32] where Rh_2MnIn and Rh_2MnTl also show similar trends. In general, our calculated values for the magnetic moments are in good agreement with other calculated values available for Type-I CoCrSb and CoMoSb [16], [13] with a minimal deviation of less than 1 %.

3.3. Electronic band structure

We performed the spin-polarized energy band structure calculations for structural phase Type-I in CoYSb (Y= Cr, Mo, W). This was carried out using the calculated equilibrium lattice constants as well as the high symmetry directions in the first Brillioun zone, as shown in Figs. 3 and 4. In both Figs. 3 and 4, the minority-spin (down) states lie within the semiconductor region and the majority (up) states in the metallic region. In Figs. 3a and 4a, the majority-spin channels energy bands exhibit metallic properties where orbitals overlap from the valence band to the conduction bands. Whereas, in the minority-spin, there is a gap separating the valence band from the conduction bands, as shown in Figs 3b and 4b. These gaps in the minority spin revealed the Half-metallic nature in CoCrSb and CoMoSb Half-Heusler alloys. For CoCrSb alloy, the valence band maximum (VBM) occurs at the Γ-point and the conduction band minimum (CBM) is located at the X-point,

Table 3: The calculated spin magnetic moments in μ_B for CoYSb (Y=Cr, Mo, W) compounds for the three possible structural phases comparing with available data.

$m^{spin}(\mu_B)$	**Calculations**	**Structural phase**	**Co**	**Y**	**Sb**	**Void**	**Tota**
CoCrSb	This work	Type I	-0.4473	2.3766	-0.0573	0.138	2.01
	other calculations		-0.36^a	2.37^a	-0.06^a		2.00^a
		Type II	-0.4917	3.0659	-0.0625	0.328	2.84
		Type III	1.1219	1.8089	-0.0177	0.01169	3.03
CoMoSb		Type I	0.6685	0.9017	-0.0148	0.2346	1.79
		Type II	1.0329	0.4100	0.0136	0.0435	1.20
		Type III	0.9274	0.0711	0.0297	0.0082	1.02
	other calculations		0.650^b	1.111^b	-0.037^b		1.82^b
CoWSb		Type I	1.0274	1.2957	-0.0285	0.1955	2.49
		Type II	0.8804	0.1896	-0.0178	0.0078	1.06
		Type III	1.6376	0.4698	0.0133	0.0293	2.15

a Ref.[16]
b Ref.[13]

resulting in an energy band gap of 0.81 eV for this alloy. This band gap is in good agreement with the previously calculated value of 0.77 eV by Zhong-Yu *et al.*[16]. Meanwhile, for CoMoSb, minority-spin gaps become broader, and the Fermi level is pushed closer to the conduction bands of the minority-spin electrons. Here, the VBM is located at the L-point, and the CBM is at the X-point, which leads to an energy band gap of 0.32 eV, as presented in Fig. 4b. This also indicates that CoMoSb is half-metallic since the alloy behaves like metal in the majority spin and shows semiconducting properties in the minority spin. We did not report on the metallic nature in CoWSb alloy because, at both majority and minority spin channels, the material has metallic properties.

To further confirm the possibility of the half-metallicity of the CoYSb (Y = Cr, Mo, W) compounds, we calculated the total spin density of state (TDOS) and spin polarization percentage for CoCrSb, CoMoSb and CoWSb, respectively. As a result, all these mentioned alloys show various degrees of half-metallic behaviours based on the spin-polarized calculation. The half-metallicity decreases from 100 % for CoCrSb to 33 % for CoWSb and further confirm half-metallicity for CoCrSb, nearly half-metallic for CoMoSb, and metallic for CoWSb as shown in table 4. The spin polarization (P) at the Fermi energy (E_F) was calculated via the following expression:

Table 4: The calculated minority-spin band gap, half-metallic (HM) gap and % spin polarization (SP) of Type I CoYSb (Y= Cr, Mo, W).

Compound	**Calculations**	**Band gap (eV)**	**HM gap (ev)**	**SP %**
CoCrSb	This work	0.81	0.21	100
	others	0.77[a]	0.22[a]	
CoMoSb		0.32		72
	others			23[b]
CoWSb				33

a Ref.[16]
b Ref.[13]

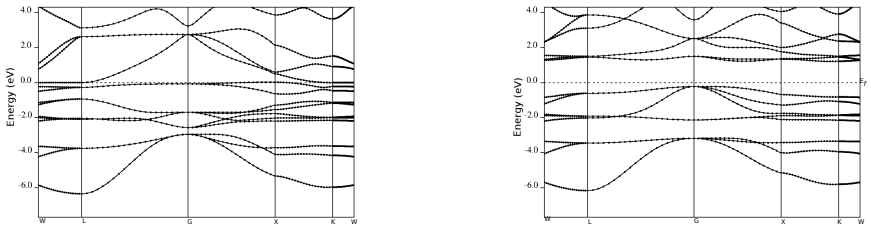

[a] [b]

Figure 3: Band structures for CoCrSb (a) majority-spin and (b) minority-spin. The Fermi level is indicated by the dashed horizontal line.

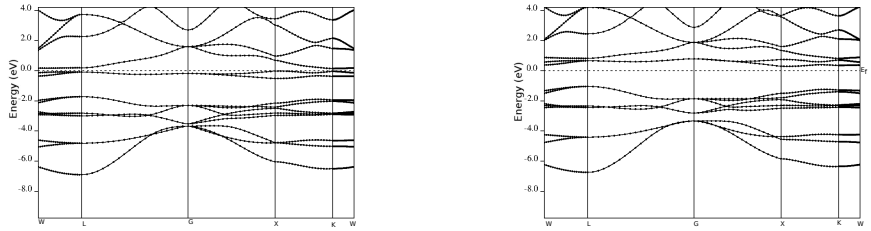

[a] [b]

Figure 4: Band structures for CoMoSb (a) majority-spin and (b) minority-spin. The Fermi level is indicated by the dashed horizontal line.

$$P = \frac{n\uparrow(E_F) - n\downarrow(E_F)}{n\uparrow(E_F) + n\downarrow(E_F)} \times 100\% \quad (1)$$

Figure 5 displays the total DOS in which for the majority-spin (up spin)

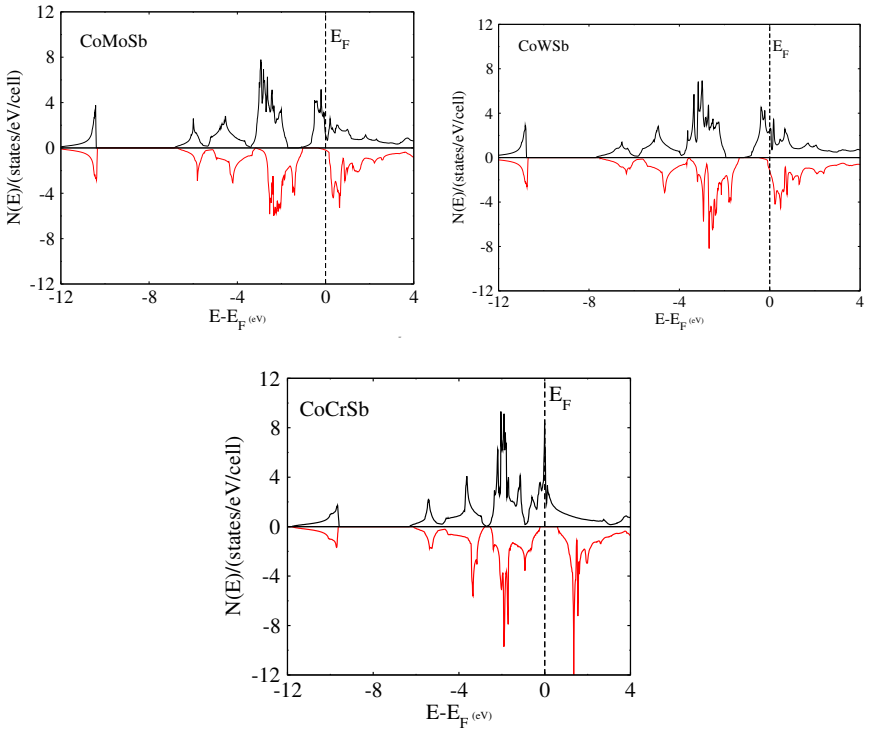

Figure 5: Calculated total spin density of states (DOS) of Type-I CoYSb alloy.

channel, the energy bands exhibit a metallic overlap with the E_F for all the alloys, whereas in the minority-spin (down spin) direction, an energy gap is opened and the E_F locates within the gap for CoCrSb, slightly close to the conduction band for CoMoSb and into the conduction band for CoWSb. Hence, CoCrSb is half-metallic (with spin polarized of 100%), CoMoSb is nearly half-metallic, and CoWSb is metallic, respectively.

3.4. Mechanical Properties

In this section, we discuss the mechanical properties and phase stability of the stable structure (Type-I), such as the elastic constants for a cubic structure which are reduced into three independent elastic constants C_{11}, C_{12}, and C_{44}, respectively. The link between mechanical and dynamic behaviour of a material such as shear modulus (G), bulk modulus (B), and young modulus (E) is usually obtained through the stress-strain method [33]. We test the mechanical stability of these compounds based on the durability of the crystal against external forces, which is a desirable property to ensure its sustain-

ability in any application. The mechanical stability is evaluated according to the Born and Huang stability criteria for cubic structure [35].

$$C_{11}>0, C_{44}>0, C_{11}-C_{12}>0, and C_{11}+2C_{12}>0. \tag{2}$$

The calculated elastic constants values for the stable Type-I structures of CoYSb (Y=Cr, Mo, and W) satisfy the above stability criteria. Hence, these compounds are mechanically stable, as shown from our results in Table 5. Furthermore, using the Voigt-Reuss-Hill approximation [36]-[37] the shear modulus (G), bulk modulus (B), Poisson's ratio (ν), and Young modulus (E) were calculated by using the following equations:

$$G = \frac{C_{11}+2C_{12}}{3} \tag{3}$$

$$B = \frac{C_{11}-C_{12}+3C_{44}}{5} \tag{4}$$

$$\nu = \frac{3B-2G}{2(3B+G)} \tag{5}$$

$$E = \frac{9BG}{3B+G} \tag{6}$$

The shear anisotropy (A), The Pugh's [34] ratio and the inverse which is Frantsevich's ratio given by the expression

$$A = \frac{2C_{44}}{C_{11}-C_{12}} \tag{7}$$

The bulk (B) and shear (G) are important in alloy applications due to the empirical rule that materials with high B and G tend to have a high melting point and high Debye temperature. Generally, B and G show how resistive alloys are when subjected to fracture and plastic deformation, respectively. The higher the value B, the more its resistance to deformation due to pressure. CoWSb resistance to pressure is stronger than that of CoMoSb and CoCrSb alloy, respectively, as shown in Table 5. The value of shear modulus G shows the resistance of a material to deformation by shear stress. The higher the value G, the higher its resistance to shear stress. Hence, CoCrSb>CoMoSb>CoWsb. The Young's modulus E characterizes the material's stiffness, and the higher the value E, the stiffer is the material.

Therefore, as shown in Table 5, CoCrSb is stiffer than CoMoSb, and CoWSb is the least stiffer. Also, the unidirectional elastic constant C_{11} is much higher than C_{44} indicating that these compounds present weaker resistance to pure shear deformation compared to resistance to unidirectional compression.

Table 5: Various mechanical properties of CoYSb (Y= Cr, Mo, W) stable phase obtained from the calculated lattice.

Calculated properties	**CoCrSb**	**CoMoSb**	**CoWSb**
C_{11} (GPa)	202.83	250.02	264.14
C_{12} (GPa)	79.61	117.98	131.46
C_{44} (GPa)	55.11	42.30	30.16
C_{11}–C_{12} (GPa)	123.22	132.04	123.68
$C_{11} + 2C_{12}$ (GPa)	362.04	485.97	527.05
B (GPa)	120.66	161.99	175.68
G (GPa)	57.63	50.59	41.61
E (GPa)	149.19	137.45	115.64
A	0.49	0.64	0.45
ν	0.29	0.36	0.39
Pugh's ratio	2.09	3.20	4.22

We also deduced the cubic Shear anisotropy factor [40] for these compounds based on equation 7. The calculated result shows anisotropy factors as 0.49, 0.64 and 0.45 for CoCrSb, CoMoSb and CoWSb, respectively. From these values, one can deduce that these compounds are substantially anisotropic in nature. The degree of ductility of a material is explained by the Pugh ratio, which is the ratio of the bulk and shear modulus of the material. The material is said to be more ductile if the Pugh's ratio increases more and it is greater than 1.75 (G/B<0.57) [41], otherwise, it is brittle. As shown in Table 5, we can see that the compounds are ductile in nature because their values are greater than 1.75. The Poisson's ratio (ν) characterises the bonding forces in material and its compression against external forces [42]-[43]. The alloys reported in this work are central-force solid (ν is generally between 0.25 to 0.5) and incompressible because ν is due to their values that lie within this range. Hence, indicating that the metallic bonding contribution to the atomic bond is dominant.

3.5. Thermodynamic Properties

The effects of temperature at constant pressure on the thermodynamic properties of the CoYSb (Y= Cr, Mo, W) material from the state equation, considering the quasi-harmonic approximation of the Debye model, were analyzed as presented below. Fig. 6 shows the behaviour of specific heat at constant volume, C_V, as a temperature function, which varied from 0 K to 800 K at constant pressure.

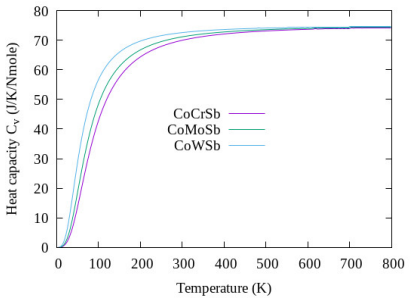

Figure 6: Heat capacity C_v against temperature for Type-I CoYSb alloy

It can be seen from Fig. 6 the trend of the specific heat towards the Dulong-Petit limit, which is the specific heat value independent of temperature. From this limit value of Dulong-Petit, as the temperature increases, each of the atoms in the material absorbs the same amount of energy proportional to the temperature increase. This value corresponds to 72.63 J/Nmol.K for CoCrSb and CoMoSb, respectively, while it reads 73.47 J/Nmol.K for CoWSb. The Debye temperature is a fundamental parameter of thermodynamic, which is linked with many physical properties of the material such as the melting temperature, lattice vibrations and specific heat at low temperature[44]. These properties listed in table 6 were obtained from the calculated elastic constants using the following equations.

$$v_l = \sqrt{\frac{3B + 4G}{3\rho}} \tag{8}$$

$$v_s = \sqrt{\frac{G}{\rho}} \tag{9}$$

Where (v_l) is the compressional velocity and (v_s) the shear sound velocity.

The average sound velocity (v_m) is expressed in terms of compressional and shear sound velocities, as stated below.

$$v_m = \left(\frac{1}{3}\right)^{1/3} \left[\frac{2}{{v_s}^3} + \frac{1}{{v_l}^3}\right] \tag{10}$$

The Debye temperature θ_D is thus expressed as

$$\theta_D = \frac{\hbar}{\kappa}\left(\frac{3n}{4\pi}\left(\frac{\rho N_A}{M}\right)\right)^{1/3} v_m \tag{11}$$

Where $\hbar$ is the reduced Planck's constant, κ is Boltzmann's constant, N_A is Avogadro's number, M is the atomic mass of a unit cell, n is the number of atomic per formula unit, and ρ is the density.

Table 6: Average sound velocity (v_m), compressional velocity (v_l), shear sound velocity (v_s), Debye temperature (θ_D) and predicted melting temperature (T_m) for the stable phase CoYSb (Y= Cr, Mo, W).

Compound	v_l **(m/s)**	v_s **(m/s)**	v_m **(m/s)**	θ_D **(K)**	T_m **(K)**
CoCrSb	5027.79	2723.03	3037.67	354.68	1751.73±300
CoMoSb	5105.36	2397.30	2688.55	308.93	2030.62±300
CoWSb	4459.49	1891.93	2113.76	243.05	2114.07±300

The Covalence bonds strength in solids is characterized by Debye temperature, which is listed in the table above along with the predicted melting temperature estimated from our elastic constant C_{11} calculated using the following expression [45].

$$T_(melting) = [555K + \left(\frac{5.91K}{GPa}\right) C_{11} \pm 300K] \tag{12}$$

Our analysis how that CoCrSb has stronger bonds than CoMoSb and CoWSb due to its higher Debye temperature.

4. Conclusions

We have investigated the structural, mechanical, electronic and thermodynamic properties of Co-based half-Heusler CoYSb (Y= Cr, Mo, W) alloys. These alloys conform to $F\bar{4}3m$ space group in the three possible atomic arrangements - the so called Type-I, Type-II and Type-III structural phases.

We determined and reported the stable atomic positions of these alloys. The optimized structures and calculated total magnetic moments show that these alloys are ferromagnetic in all three phases. Electronic band structures analysis show that CoCrSb and CoMoSb are half-metallic and nearly half-metallic, respectively in nature. This is complemented with their percentage of spin polarization and confer to these materials potential uses in spintronic. We also confirmed their mechanical stability and predicted their anisotropy.

References

[1] D. Kieven, R. Klenk, S. Naghavi, C. Felser, and T. Gruhn, Phys. Rev. B 81, 075208 (2010).

[2] S. Wurmehl, G. H. Fecher, H. C. Kandpal, V. Kseno-fontov, C. Felser, H. J. Lin and J. Morais, Phys. Rev. B 72, 184434 (2005).

[3] S. A. Wolf, D. D.Awschalom, R. A.Buhrman, J. M.Daughton, S.von Molnar, M. L.Roukes, A. Y. Chtchelkanova and D. M. Treger, Science 294: 1488-1495 16 NOVEMBER 2001.

[4] A. Roy, J. W. Bennett, K. M. Rabe, and D. Vanderbilt, Phys. Rev. Lett. 109, 037602 (2012).

[5] D. Xiao, Y. Yao, W. Feng, J. Wen, W. Zhu, X.Q. Chen, G.M. Stocks, and Z. Zhang, Phys. Rev. Lett. 105 (2010), p. 096404.

[6] H. Lin, L.A. Wray, Y. Xia, S. Xu, S. Jia, R.J. Cava, A. Bansil, and M.Z. Hasan, Nat. Mater. 9 (2010), pp. 546–549.

[7] M. Zeeshan, H.K. Singh, J. Van den Brink and H. C. Kandpal, Phys. Rev. Mater. 1 (2017) 075407.

[8] S. D Li, Z. R Yuan, L.Y. Lu, M.M. Liu, Z.G. Huang, F. M Zhang, Y.W. Du, Mater. Sci. Eng., A 428 (2006) 332.

[9] P. Larson, S. D. Mahanti, and M. G. Kanatzidis, Phys. Rev.B 62, 12754 (2000).

[10] F. B. Mancoff, J. F. Bobo, O. E. Richter, K. Bessho, P. R. Johnson, R. Sinclair, W. D. Nix, R. White, and B. M. Clemens, J. Mater. Res. 14, 1560 (1999).

[11] R. A. de Groot, F. M. Mueller, P. G. van Engen, and K. H. J. Buschow, Phys. Rev. Lett. 50, 2024 (1983).

[12] I. Galanakis, P. Mavropoulos, and P. H. Dederichs, J. Phys. D 39, 765 (2006).

[13] B.R.K. Nanda and J. I Dasgupta, Phys. Condens. Matter 15 (2003) 73077323.

[14] S. Minami, I. Fumiyuki, M. P. Yo and S. Mineo, AIP: Applied Physics Letter 113, 032403.

[15] H.C.Kanpal, C. Felse and R. Seshadri, J. of phys. D: App. Phys. 39, 776.

[16] Y.Zhong-Yu, S. Li, P. Meng-Mei and S. Shu-Juan, Acta Phys. Sin. Vol. 65, No. 12 (2016) 127501.

[17] J. Tobola and J. Pierre, J. Alloys Compd. 296, 243 (2000).

[18] S. E Kulkova, S. V Eremeev, T. Kakeshita, S. S Kulkov and G. E Rudenski, mater. Trans. Vol 47, No 3 (2006) 604.

[19] R. W. G. Wyckoff, Crystal Structures, 2nd ed., Vol. 1 (John Wiley and Sons, 1963).

[20] F. D. Murnaghan, Proc. Natl. Acad. Sci. USA. 30 (1944) 244.

[21] B. Hillebrands, C. Felser, J. Phys. D: Appl. Phys. 39 (2006) 5.

[22] T. Graf, C. Felser, S.S.P. Parkin, Progr. Solid State Chem. 39 (1) (2011) 1–50.

[23] I. Galanakis, K. Ozdogan, E. Sasioglu, B. Aktas, Phys. Rev. B 75 (2007) 172405.

[24] S. Scandolo, P. Giannozzi, C. Cavaoni, S. de Gironcoli, A. Pasquarello and S. Baroni, Z. Kristallogr, 220 (2005) 574579.

[25] P. Giannozzi, S. Baroni, N. Bonini, M. Calandra, R. Car, C. Cavazzoni, D. Ceresoli, G. L. Chiarotti, M. Cococcioni, I. Dabo, A. D. Corso, S. de Gironcoli, S. Fabris, G. Fratesi, R. Gebauer, U. Gerstmann, C. Gougoussis,

A. Kokalj, M. Lazzeri, L. Martin-Samos, N. Marzari, F. Mauri, R. Mazzarello, S. Paolini, A. Pasquarello, L. Paulatto, C. Sbraccia, S. Scandolo, G. Sclauzero, A. P. Seitsonen, A. Smogunov, P. Umari, R. M. Wentzcovitch, J. Phys.:Condens. Matter 21 (39) (2009) 395502.

[26] P. Giannozzi, O. Andreussi, T. Brumme, O. Bunau, M. Buongiorno Nardelli, M. Calandra, R. Car, C. Cavazzoni, D. Ceresoli, M. Cococcioni, N. Colonna, I. Carnimeo, A. Dal Corsol, S. de Gironcoli, P. Delugas, R. A. DiStasio Jr, A. Ferreti, A. Floris, G. Fratesi, G. Fugallo, R. Gebauer, U. Gerstmann, C. Gougoussis, F. Giustino, T. Gorni, J. Jia, M. Kawamura, H. Y Ko, A. Kokalj, E. Kkbenli, M. Lazzeri, M. Marsili, N. Marzari, F. Mauri, N. L. Nguyen, H. V. Nguyen, A. Otero-de-la-Roza, L. Paulatto, S. Ponc, D. Rocca, R. Sabatini, B. Santra, M. Schlipf, A. P. Seitsonen, A. Smogunov, I. Timrov, T. Thonhauser, P. Umari, N. Vast, X. Wu and S. Baroni. 2017 J. Phys.: Condens. Matter 29 465901.

[27] J. P. Perdew, K. Burke, and M. Ernzerhof, Phys. Rev. Lett. 77 (1996) 3865.

[28] https://dalcorso.github.io/thermopw

[29] A. Dal Corso, J. of Phys.: Condens. Matter 28 (2016) 075401.

[30] H. J. Monkhorst and J. D. Pack, Phys. Rev. B 13 (1976) 5188.

[31] J. Kubler, Phys. B+C 127 (1984) 257.

[32] I. Galanakis, P. H Dederichs and P. H Mavropoulous: Phys. Rev. B 66 (2002) 174429.

[33] Y. Le Page and P. Saxe, Phys. Rev. B. 65 (2002) 104104.

[34] S. F. Pugh, Philos. Mag. 45 (1954) 823.

[35] M. Born and K. Huang, Dynamical Theory of Crystal Lattices (Oxford: Oxford Clarendon Press, 1956), pp 120-156.

[36] W. Voigt, Lehrbuck der Kristallphysik (B. B. Teubner, Leipzig, 1928), pp 739.

[37] H. B. Huntington, Solid State Physics, F. Seitz and D. Properties of Engineering Ceramics, W. Kriegel and H. Palmour, Turnbull, Eds. (Academic Press Inc., New York, 1958), Vol. 7

[38] A. Reuss, Z. Angew, Math. Mech. 9 (1929) 49.

[39] R. Hill, Proc. Phys. Soc. (London) 65 (1952) 349.

[40] C. Zener, Elasticity and Anelasticity of Metals, University of Chicago Press, Chicago, 1948.

[41] A. R. Degheidy, E. B. Elkenany, Chin. Phys. 26 (2017) 086103.

[42] D. C. Gupta and S. Ghosh, J. Magn. Magn. Mater. 435 (2017), pp. 107-116.

[43] H. Fu, D. Li, F. Peng, T. Gao, and X. Cheng, Comput. Mater. Sci. 44 (2008), pp. 774-778.

[44] O.L. Anderson, J. Phys. Chem. Solids 24 (1963) 909.

[45] M.E. Fine, L.D. Brown, and H.L. Marcus, Scr. Metall. 18 (1984), pp. 951–956